

Impacts of Capillary Pressure Imbibition Curves on the Simulation of Waterfloods in High Capillary Moderately-Water-Wet Chalk

Bognø, T., Graue, A.

University of Bergen, Bergen, Norway

Abstract

Iterative comparison between experiments and numerical simulations may be used to predict oil recovery mechanisms in oil reservoirs. In-situ fluid saturation data, capillary pressure and relative permeability curves are important input parameters in the simulations. By individually optimising P_c -data or k_r -curves in the simulations of the oil production and the in-situ fluid saturation dynamics in the experiments, it is possible to validate experimental input parameters, evaluate their impact on the simulations and determine what oil recovery mechanisms are most important.

Capillary pressure is one of the most important input parameters to numerical simulations of waterfloods in high capillary chalk. Extensive efforts have therefore been dedicated to improve experimental measurements of the capillary pressure at various wettabilities to understand and thus improve oil recovery. In this paper experimental capillary pressure data on the positive part of the capillary pressure imbibition curve has been measured by the Direct Measurement of Saturation (DMS) method.

The objective of this work was to illustrate the impact of the positive part of the capillary pressure imbibition curve in waterfloods of moderately-water-wet chalk. Numerical simulations demonstrate how various shapes of the positive part of the capillary pressure imbibition curve influenced the oil recovery and the in-situ fluid saturation development. The physical interpretation of the recovery mechanisms is assisted by comparing various realisations of the numerical simulations using different shapes of the positive part of the capillary pressure imbibition curve.

Introduction

Laboratory waterflood experiments, using larger blocks of chalk, where the advancing waterfront has been imaged by a nuclear tracer technique showed that changing the wettability conditions from strongly-water-wet to moderately-water-wet had minor impact on the oil production, both in fractured and non-fractured physical reservoir models.¹⁻³ The in-situ fluid saturation development, however, was significantly different when fractures were present, indicating differences in oil recovery mechanisms.⁴

We have earlier reported on a technique that reproducibly alters wettability in outcrop chalk by aging the rock material in stock tank crude oil at elevated temperature for a selected period of time.⁵ After applying this aging technique on several blocks of chalk we have imaged waterfloods on blocks of outcrop chalk at different wettability conditions, first as a whole block, then when the blocks were fractured and reassembled.^{4,6,7}

In this work the validity the experimentally measured capillary pressure and relative permeability data, used as input for the simulator, has been tested at moderately-water-wet

conditions. The term moderately-water-wet in this paper is defined to cover the wettability conditions reflecting an Amott-Harvey water index, I_w , in the range 0.5 – 0.8. Optimization of either P_c -data or k_r -curves for moderately-water-wet chalk in the numerical simulations of the whole blocks gave indications of the validity of the experimental data. History matching both the production profile and the in-situ fluid saturation distribution development gave higher confidence in the simulations than matching the effluent profile only. Keeping endpoint saturations constant, various shapes of the positive part of the imbibition capillary pressure curve were tested in the numerical model.

Experimental

Rock Material and Preparation

The chalk block, CHP8, approximately $20 \times 12 \times 5$ cm, was obtained from a large piece of Rørdal outcrop chalk from the Portland quarry near Ålborg, Denmark. The block was cut to size with a band saw and used without cleaning. Local air permeability was measured at each intersection of a 1×1 cm grid on both sides of the blocks using a minipermeameter. The measurements indicated homogeneous block on a cm scale. This chalk material had never been contacted by oil and was strongly water-wet. The block was oven dried for three days at 90°C . End pieces were mounted on the block and the whole assembly was epoxy coated. Each end piece contained three fittings so that entering and exiting fluids were evenly distributed with respect to height. The block was vacuum evacuated and saturated with brine containing 5 wt% NaCl + 3.8 wt% CaCl_2 . Fluid data is found in Table 1. Porosity was determined from weight measurements and the permeability was measured across the epoxy coated block, at $2 \cdot 10^{-3} \mu\text{m}^2$ for CHP8, see block data in Table 2.

Immobile water saturations of 28%PV were established for the block by oilflooding. To obtain uniform initial water saturation, S_{wi} , oil was injected alternately at both ends. Oilflood of the epoxy coated block, CHP8, are carried out using stock tank crude oil in a heated pressure vessel at 90°C with a maximum differential pressure of 135 kPa/cm.

Wettability Alteration

Selective and reproducible alteration of wettability, by aging in crude oil at elevated temperature, produced a moderately-water-wet chalk block. Block CHP8 was aged in crude oil at 90°C for 83 days at an immobile water saturation of 28%PV. A North Sea crude oil, filtered at 90°C through a chalk core, was used to oilflood the block and for the aging process. Two twin samples drilled from the same chunk of chalk that the block was cut from, were treated similar to the block. An Amott-Harvey test was performed on these samples to indicate the wettability conditions after aging.⁸ After the waterflood were terminated, four core plugs were drilled out of the block and wettability measurements using the Amott-Harvey test were conducted.

Because of possible wax problems with the North Sea crude oil used for aging, decane was used as the oil phase during the waterflood, which were performed at room temperature. After the aging was completed for CHP8 the crude oil was therefore flushed out with decahydronaphthalene (decalin), which again was flushed out with n-decane, all at 90°C . Decalin was used as buffer between the decane and the crude oil to avoid asphaltene precipitation, which may occur when decane contacts the crude oil.

Saturation Determination

2-D brine saturations were determined using a flow rig, which was designed and built at the University of Bergen, to measure gamma ray emission from ^{22}Na dissolved in the brine.

Although CaCl_2 was in the brine to buffer Na adsorption, several pore volumes of non-radioactive brine was initially flushed through the block to minimize potential adsorption of the radioactive tracer, $^{22}\text{NaCl}$, before the rock was exposed to the radioactive brine.

The rig held the block in a vertical position and measured the radiation in the x-y plane over the block to produce a saturation map at each specified point in time. Radiation detection, i.e. saturation measurement, during the waterflood was made at the intersections in a 1×1 cm grid. The working principle of this nuclear tracer technique has been described in detail elsewhere.^{6,7}

To prevent counter current imbibition from producing oil into the water inlet, a low differential pressure, initially less than 1.5 kPa, was applied across the block during the constant flow rate waterflood. The injection flow rates are included in Table 2.

The outline of the experimental sequence used to waterflood the block, while using 2-D imaging to determine the distribution of brine saturation, is summarized in Table 2.

Results and Discussion

Block CHP8 was, after subsequent oilfloods, waterflooded three times, first as a whole block, then with an embedded fracture network and finally with an interconnected fracture network. This discussion will emphasise the comparison of the experimental and simulation results of the waterflood of the whole block. Results on the waterfloods of the block when fractured are reported in Ref. 9.

Wettability Tests

To obtain a measure of the wettability conditions of CHP8, after aging a duplicate set of core plugs, PC2-13 and PC2-15 were used. The plugs were aged similarly to the block and then cooled to room temperature, after the crude oil was exchanged with decalin and decane. Oil recovery by spontaneous room temperature imbibition, followed by a waterflood, were performed on the aged core plugs, producing the Amott water index, I_w .⁸ Core plug history and results are found in Table 3 in Ref. 10. In Fig. 1 the imbibition characteristics for the core plugs are shown, where for comparison imbibition characteristics for some Rørdal chalk core plugs at strongly-water-wet and nearly-neutral-wet conditions are included. Imbibition rate and endpoint saturation after spontaneous imbibition decreased with increased aging time corresponding to a consistent change towards a less-water-wet state. Repeated imbibition tests on the core plugs after aging confirmed stable wettability conditions. The measured wettability index to water, I_w , for the two plugs were recorded at 0.52 and 0.54, respectively. The Amott-Harvey test was conducted three times on these samples to verify stability and reproducibility in the measurements. The second wettability test was performed with iododecane as the oil phase, needed in a subsequent steady-state relative permeability test using a Penn-State technique with X-ray attenuation imaging, to generate input for numerical simulations. The third wettability test was performed after the samples had been transported back and forth between Bergen, Norway, and Houston, Texas, where the relative permeability tests were performed by a service company.¹⁰

Waterflood of Whole Block CHP8

Results from waterfloods of whole blocks, both at strongly-water-wet conditions and at moderately-water-wet conditions have earlier been shown to be similar with respect to in-situ fluid saturations.⁴ The dynamics of the in-situ water saturation for the waterflood of whole block CHP8, is shown in Fig. 2. The individual saturation maps are identified by a scan number. Each scan number was preceded by a letter and number to identify the block, e.g. P8

for CHP8. The code for the scans are as follows: The oil and water floods were labeled O and W, respectively, with the first digit being the flood number and the two digits following the dash indicating the chronological sequence of the scan. Thus, P8W1-09 is the 9th scan of the 1st water flood on block CHP8.

In the waterflood experiment the brine was injected from the left side of the image and the displaced fluids exited at the right side of the image.

A uniform initial water saturation was measured for CHP8 as the first saturation map, P8W1-01 in Fig. 2. Scan P8W1-01 to Scan P8W1-42, show a slightly higher brine saturation at the bottom of the block near the inlet, suggesting a gravitational effect in the vertical brine distribution across the block. This could be due to the slightly higher pressure at the lower part of the block caused by the higher water head in the injection end piece, however, these were very small pressure differences, ca. 1.0 kPa.

A dispersed waterfront flushed out 45%PV of the decane. Increasing the flow rate has been shown to produce a less dispersed waterfront.¹ In waterfloods starting at higher initial water saturations there was essentially no waterfront at all, a uniform increase in water saturation was recorded.⁶ A uniformly distributed final water saturation was obtained for all of the tests.

Capillary Pressure and Relative Permeability

We have earlier measured the capillary pressure and relative permeabilities in chalk core plugs at strongly-water-wet, moderately-water-wet and nearly-neutral-wet conditions.¹⁰ Plug wettability was selectively altered by aging outcrop chalk plugs, at Swi, in crude oil at an elevated temperature for selected periods of time. This procedure reproduced the desired wettability while keeping the pore network structure and the mineralogy constant. Aging to a less-water-wet state significantly reduced spontaneous brine imbibition rate and endpoint. However, it did not reduce the total movable oil, i.e. imbibition plus forced displacement. In fact, the total movable oil generally increased slightly with reduced water wettability, however, at the cost of higher differential pressures. Reduced water wettability also lowered the drainage threshold pressure. Repeated imbibition tests on individual plugs indicated that the wettability alteration was permanent. These tests were conducted in order to provide experimentally obtained input data for capillary pressure and relative permeability at a range of wettability conditions for numerical simulations of the waterflood of the block.

Numerical Simulations

A full field numerical reservoir simulator SENSOR, was used in black oil mode to simulate the waterflood experiment on the whole block CHP8.

The first simulations were run using the experimentally measured values for capillary pressure and relative permeabilities at the different wettabilities. To improve the history matches for both the oil production and the dynamics of the in-situ fluid saturations, optimization of capillary pressure curves was carried out keeping the relative permeabilities from the core analysis results constant, and then vice versa, using the capillary pressure from the centrifuge measurements and optimize the relative permeabilities. This procedure would also give information on which of the measured values could be most trusted.

Figures 3 and 4 exhibit the results from simulating the waterfloods of the moderately-water-wet whole block CHP8. The overall best match with the experiment was obtained using the experimentally obtained capillary pressure curves and optimizing the relative permeabilities. An excellent match was obtained for the oil production, but the match of the in-situ fluid saturation development was unsatisfactory.

When the waterfloods were completed, the experimental results on the wettability measurements of the core plugs drilled out of the blocks became available, see Table 3. In Figure 5 the spontaneous imbibition characteristics of these core plug samples are compared to the duplicate set of plugs used earlier. The results reveal that the aging process in the epoxy coated block CHP8 was slower than for the twin samples submerged in crude oil, leaving the block at a wettability index to water, $I_w=0.8$, rather than at $I_w=0.5$ as indicated by the twin samples. This has later been shown to be an artifact of the practical arrangement during aging.¹¹ The interaction with the numerical simulations, corresponding to applying a modified and more water-wet capillary pressure curves, gave a better match with the experiments in particular with the in-situ fluid saturation development, see Figures 6 and 7.

Figure 8 shows the experimentally measured relative permeability curves compared to the optimized curves obtained for the history match of the whole block CHP8. Figure 9 shows the capillary pressure curves for the chalk matrix as measured at the moderately-water-wet conditions and the modified curves at $I_w=0.8$ used after it came apparent that the block was more water-wet than first indicated by comparison with the twin samples. The positive pressure part of the imbibition capillary pressure curve at $I_w=0.5$ was obtained by the Direct Measurement of Saturation method from similar core plugs.^{12,13}

Due to lack of accurate information on the positive portion of the capillary pressure imbibition curve for the wettability $I_w = 0.8$, three realizations for the numerical simulation of the whole block CHP8 waterflood were performed using three different representations of the positive capillary pressure curve representing the spontaneous imbibition process (Figure 10). The relative permeabilities were optimized for each representation. This procedure should indicate which of the capillary pressure curves would best represent the capillary forces at moderately-water-wet conditions, $I_w = 0.8$. This procedure was meant also as a test of the interpretation of the significance of the spontaneous imbibition on the recovery mechanism at moderately-water-wet conditions. If the higher or the medium capillary pressure curves, indicated in Figure 10, would give the best history match, the capillary forces would accordingly be more dominant during the oil displacement at lower water saturations. If the lower capillary pressure curve gave the best match, the viscous forces would be dominant and assist in the displacement of mobile oil.

For the higher capillary pressure imbibition curve we kept the P_c -value high even near the endpoint for spontaneous imbibition to reflect an abrupt drop in capillary pressure sometimes experienced near the endpoint for spontaneous imbibition in water-wet high capillary chalk. This might be interpreted as when the non-wetting phase becomes discontinuous and trapped. This has previously been observed during capillary pressure measurements at strongly-water-wet conditions using the Direct Measurement of Saturation method.¹³ Figures 11 and 12 show the results from the best history match of the waterflood of the whole block CHP8. The medium capillary pressure curve from Figure 10 turned out to give the best overall match with the experimental results.

Conclusions

- Two-dimensional in-situ saturations during waterfloods at moderately-water-wet conditions in a large block of chalk have been monitored and used to determine oil recovery mechanisms at different wettability conditions.
- Experimentally obtained P_c and k_r -input data to the simulator have been evaluated by history matching in-situ fluid saturation dynamics and oil production.

- The overall best match between the simulations and the experiments was obtained using the experimentally determined capillary pressure curves and optimizing the relative permeabilities.
- Through numerical simulations the capillary pressure imbibition curve assisted in determining the wettability and oil recovery mechanisms in chalk at moderately-water-wet conditions.
- The shape of the positive portion of the capillary pressure imbibition curve gave significant impacts on the history match of in-situ fluid dynamics in waterfloods in moderately-water-wet chalk, while the total oil recovery was not affected.

References

1. Lien, J.R., Graue, A., Kolltveit, K.: "A Nuclear Imaging Technique for Studying Multiphase Flow in a Porous Medium at Oil Reservoir Conditions," Nucl. Instr. & Meth., A271, 1988.
2. Graue, A., Kolltveit, K., Lien, J.R., Skauge, A.: "Imaging Fluid Saturation Development in Long Coreflood Displacements," *SPEFE*, Vol. 5, No. 4, 406-412, Dec. 1990.
3. Graue, A.: "Imaging the Effect of Capillary Heterogeneities on Local Saturation Development in Long-Core Floods," *SPEDC*, Vol. 9, No. 1, March 1994.
4. Graue, A., Viksund, B.G., Baldwin, B.A., Spinler, E.: "Large Scale Imaging of Impacts of Wettability on Oil Recovery in Fractured Chalk," *SPE Journal*, Vol. 4, No. 1, March 1999.
5. Graue, A., Viksund, B.G., Baldwin, B.A.: "Reproducible Wettability Alteration of Low-Permeable Outcrop Chalk," *SPE Res. Eng. and Eval.*, April, 1999.
6. Viksund, B.G., Graue, A., Baldwin, B., Spinler, E.: "2-D Imaging of waterflooding a Fractured Block of Outcrop Chalk," Proc.: 5th Chalk Research Symposium, Reims, France, (Oct. 7-9, 1996).
7. Viksund, B.G., Eilertsen T., Graue, A., Baldwin, B., Spinler, E.: "2D-Imaging of the Effects from Fractures on Oil Recovery in Larger Blocks of Chalk," Reviewed Proc.: International Symp. of the Society of Core Analysts, Calgary, Canada. (Sept. 8-10, 1997).
8. Amott, E.: "Observations Relating to the Wettability of Porous Rock," *Trans.*, AIME 1959 216, 156-162.
9. Graue, A., Bognø, T.: "Wettability Effects on Oil Recovery Mechanisms in Fractured Reservoirs," SPE 56672, 1999 SPE Annual Tech. Conf. And Exh., Houston, TX, Oct. 3-6, 1999.
10. Graue, A., Bognø, T., Moe, R.W., Baldwin, B.A., Spinler, E.A., Maloney, D., Tobola, D.P.: "Impacts of Wettability on Capillary Pressure and Relative Permeability," presented at the 1999 International Symposium of Core Analysts, Golden, Co., USA, Aug., 1999.
11. Graue, A., Aspenes, E., Bognø, T., Moe, R.W., Ramsdal, J.: "Alteration of Wettability and Wettability Heterogeneity," Reviewed Proc., 6th International Symposium on Evaluation of Reservoir Wettability and Its Effect on Oil Recovery, Socorro, NM, USA, Sept. 27-28, 2000.
12. Baldwin, B.A., Spinler, E.A.: "A Direct Method for Simultaneously Determining Positive and Negative Capillary Pressure Curves in Reservoir Rock," *Journal of Petroleum Science and Engineering* (1998) 20, 161-165.
13. Bognø, T., Aspenes, E., Graue, A., Spinler E.A., Tobola, D.: "Comparison of Capillary Pressure Measurement at Various Wettabilities Using the Direct Measurement of Saturation Method and Conventional Centrifuge Techniques," presented at the 2001 International Symposium of Core Analysts, Edinburgh, Scotland, 17-19 Sep., 2001.

SI Metric Conversion Factors

cp × 1.0*	E-03 = Pa·s
ft × 3.048*	E-01 = m
ft ² × 9.290 304*	E-02 = m ²
ft ³ × 2.831 685	E-02 = m ³
in. × 2.54*	E+00 = cm
lbf × 4.448 222	E+00 = N
mD × 9.869 233	E-04 = μm ²
psi × 6.894 757	E+00 = kPa

*Conversion factor is exact

Table 1. Fluid properties.

Fluid	Density [g/cm ³]	Viscosity [cP] at 20°C	Viscosity [cP] at 90°C	Composition
Brine	1.05	1.09		5 wt% NaCl + 3.8 wt% CaCl ₂
n-Decane	0.73	0.92		
Decahydronaphtalene	0.896			
Crude oil	0.849	14.3	2.7	

Table 2. Experimental data for chalk blocks.

Block	CHP 8		
Outcrop	Portland		
Location	Ålborg		
Length (cm)	19.9		
Height (cm)	10.0		
Thickness (cm)	5.5		
Abs. Permeability (mD)	2.3		
Porosity (%)	47.6		
Pore Volume (ml)	516		
MISC. FLOOD # :	1		
Flow Rate (ml/hr)	10		
OILFLOOD # :	1	2	3
Oil Viscosity (cP)	2.7	0.92	0.92
S _{wi} (%PV)	100	76	72
DS _w (%PV)	72	43	37
S _{wf} (%PV)	28	33	35
Max Pressure (Bar)	10	24	24
Endpoint Eff. Perm. (mD)	3 ^c	1.3 ^a /1.3 ^b	1.0 ^a /42 ^b
AGING :	YES		
Aging Temp. (°C)	90		
Aging Time (days)	83		
Amott index after aging (measured on samples)	0.54		
Oil flooding prior to imb. :			
Decaline (PV)	5		
n-Decane (PV)	5		
Endpoint eff. Perm. (mD)	2.4		
WATERFLOOD # :	1	2	3
Block Condition	Whole	Fractured	Fractured
Cutting	XX	Band Saw	Band Saw
Oil Viscosity (cP)	0.92	0.92	0.92
S _{wi} (%PV)	28	33	35
DS _w (%PV)	45	39	40
S _{wf} (%PV)	73	72	75
Max Pressure (Bar)	XX	XX	XX
Endpoint eff. Perm. (mD)	0.4	0.2	0.3
Oil Recovery (%OIP)	63	58	62
Flow Rate (ml/hr)	1	1	1

a) Whole Block

b) Fractured block

c) End point relative permeability tends to be higher than the absolute permeability.

Table 3. Experimental history for drilled-out plugs.

Core	CHP8-1	CHP8-2	CHP8-4
Drilled from block #	CHP8	CHP8	CHP8
Outcrop	Portland	Portland	Portland
Location	Denmark	Denmark	Denmark
Lenght (cm)	5.2	5.3	5.3
Diameter (cm)	3.7	3.7	3.7
Porosity (%)	48	48	48
Pore Volume (ml)	27	27	27
Abs. Permeability (mD)	2	2	2
Oilflood #	1	1	1
Oil Viscosity (cP)	2.7	2.7	2.7
S_{wi} (%PV)	75	75	75
DS_w (%PV)	39	39	44
S_{wf} (%PV)	36	36	31
Spontaneous Imbibition #	1	1	1
Oil Viscosity (cP)	0.92	0.92	0.92
S_{wi} (%PV)	36	36	31
DS_w (%PV)	35	30	39
S_{wf} (%PV)	71	66	70
Oil Recovery (%OIP)	55	47	56
Water Flood #	1	1	1
Flow Rate (ml/hr)	34	34	34
S_{wi} (%PV)	71	66	70
DS_w (%PV)	10	5	8
S_{wf} (%PV)	81	71	78
Recovery (%OIP)	70	55	68
End point Eff. Perm. (mD)	0.8	1	1
Wettability Index	0.79	0.86	0.82

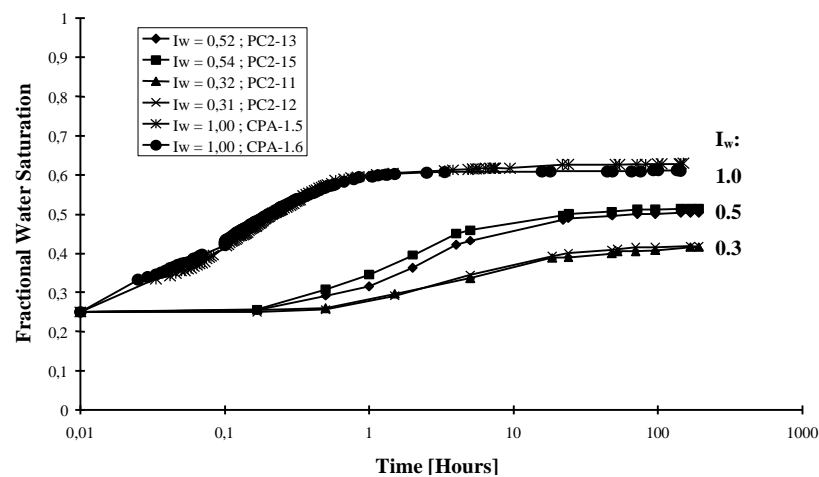


Figure 1. Spontaneous imbibition characteristics for Rørdal chalk plugs at different wettabilities.

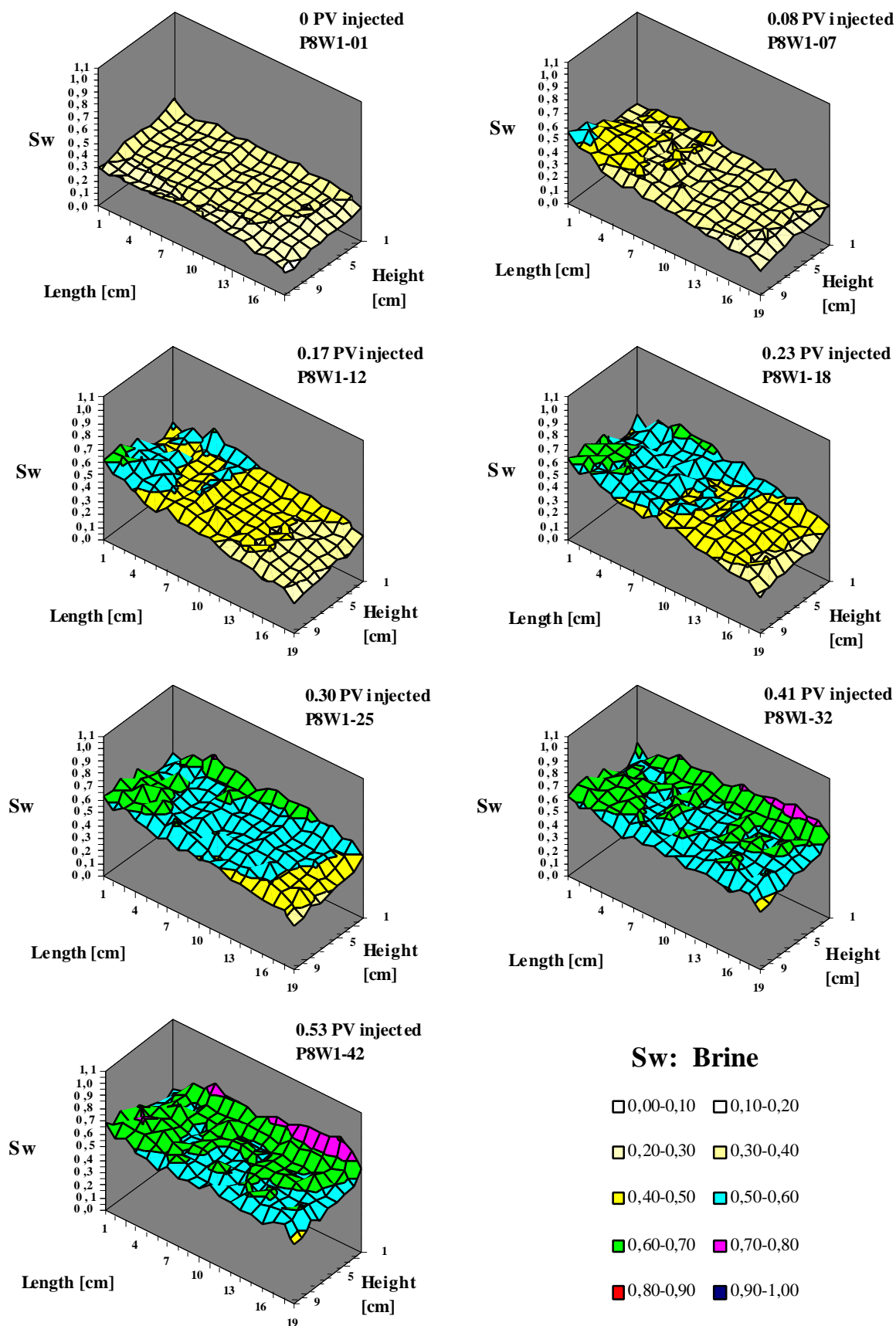


Figure 2. In-situ saturation development for the waterflood of whole block CHP8.

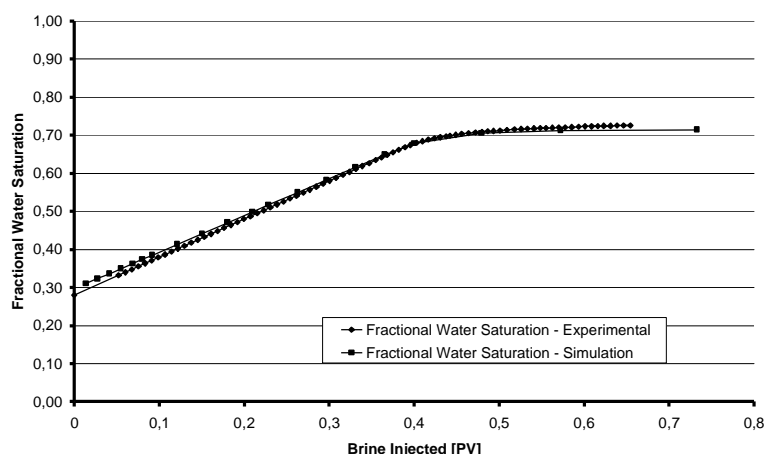


Figure 3. Comparison of experimental and simulated average water saturations when waterflooding the whole block CHP8. Optimized experimentally measured relative permeability curves and experimental capillary pressure curves are used in the simulations.

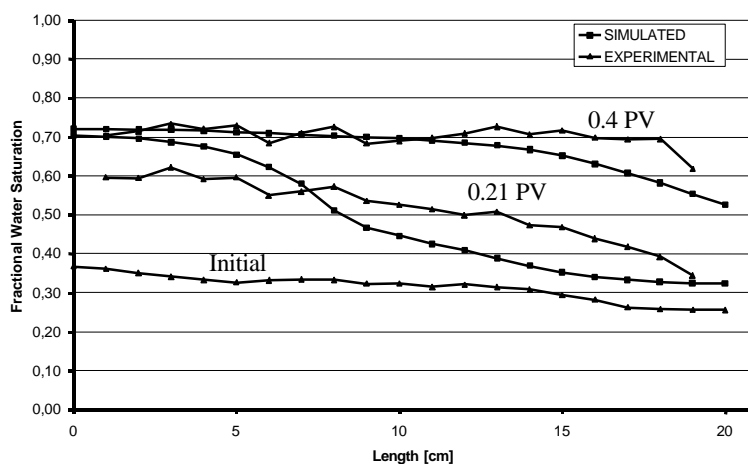


Figure 4. Comparison of experimental and simulated water saturation profiles averaged over cross section of block, at three time steps, when waterflooding the whole block CHP8. Optimized experimentally measured relative permeability curves and experimental capillary pressure curves are used in the simulations.

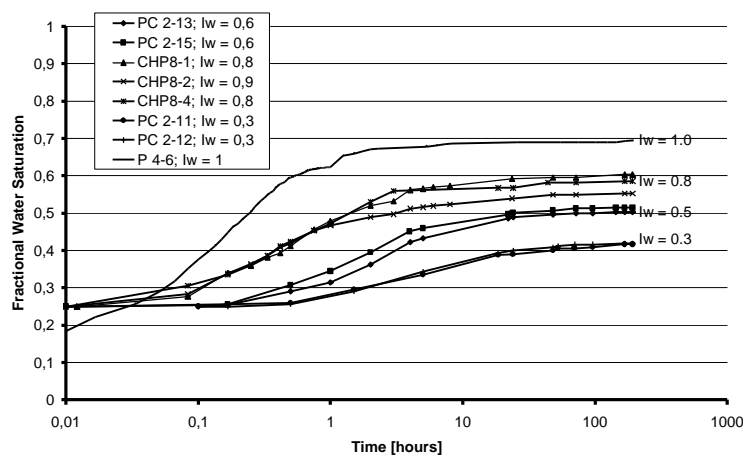


Figure 5. Imbibition characteristics for duplicate set of core plugs, PC2-13 and PC2-15, and drilled-out plugs, CHP8-1 to 4, from the moderately-water-wet block CHP8. Corresponding data for strongly-water-wet and nearly-neutral-wet plugs are included for comparison.

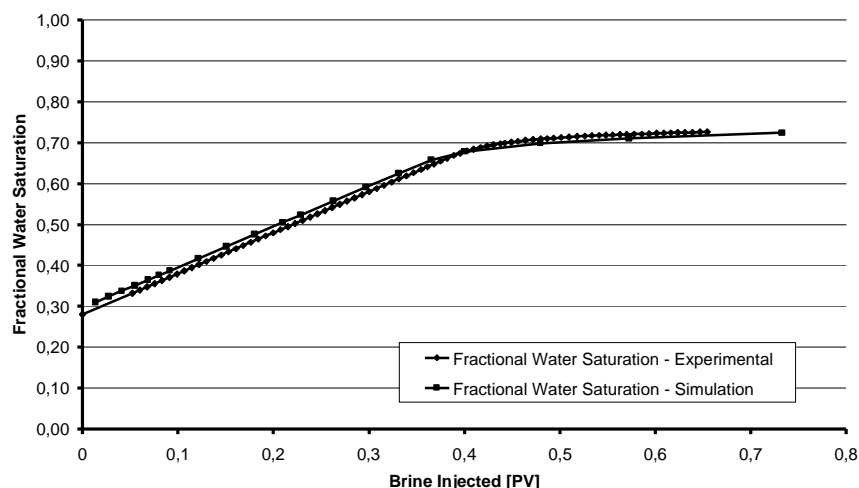


Figure 6. Experimental and simulated average water saturations when waterflooding the whole block CHP8. A modified capillary pressure curve is used in the simulations.

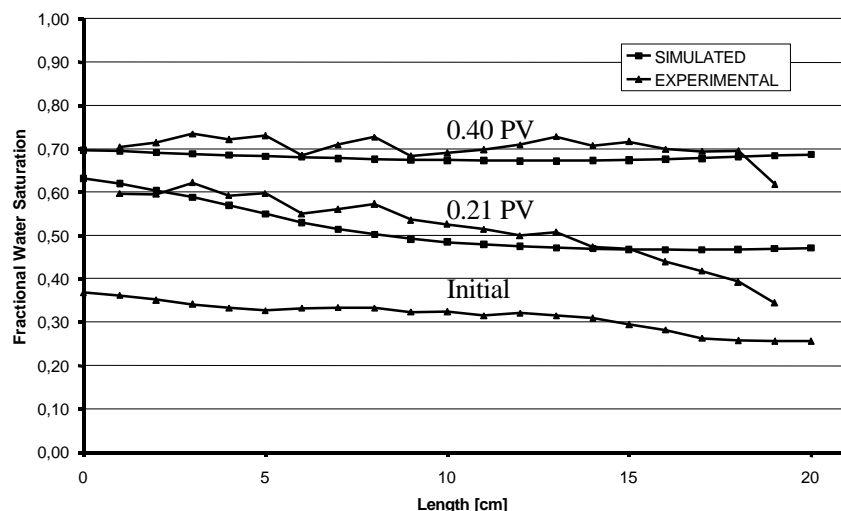


Figure 7. Experimental and simulated water saturation profiles averaged over cross section of block, at three time steps, when waterflooding whole block CHP8. Simulations with modified, $I_w=0.8$, capillary pressure curve.

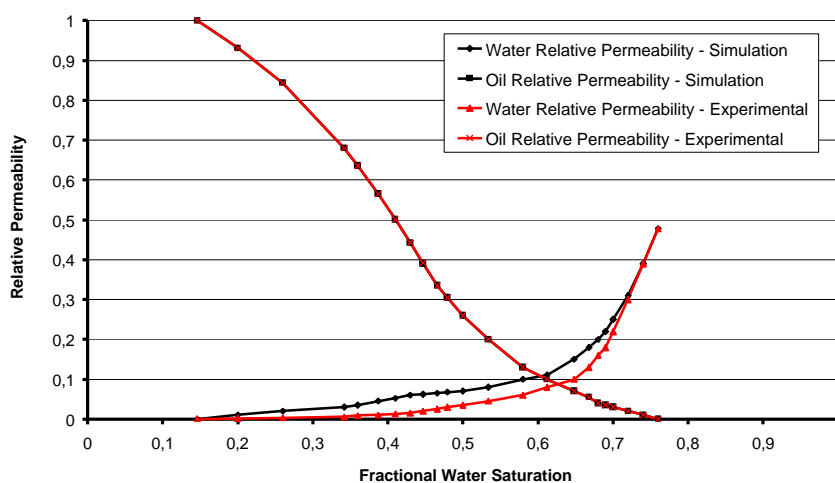


Figure 8. Experimentally obtained relative permeability curves compared to optimized relative permeability curves during history matching the waterfloods of the whole block CHP8.

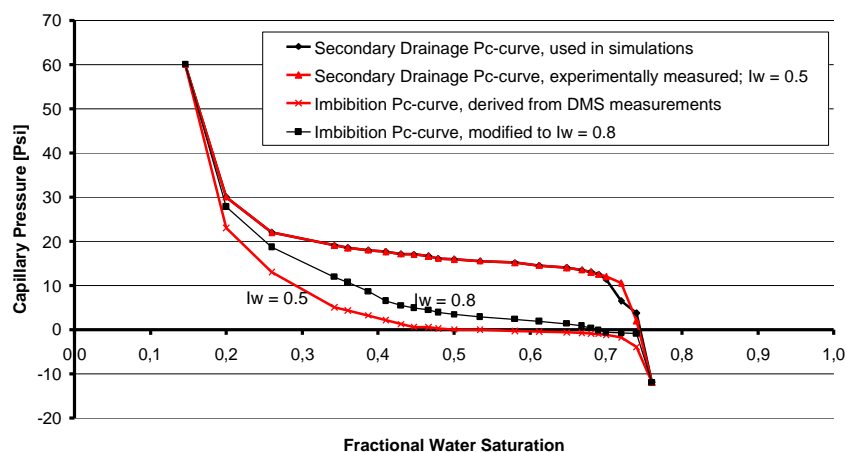


Figure 9. Experimentally obtained capillary pressure curves compared to the modified capillary pressure curves, $I_w=0.8$, used for input to the simulator.

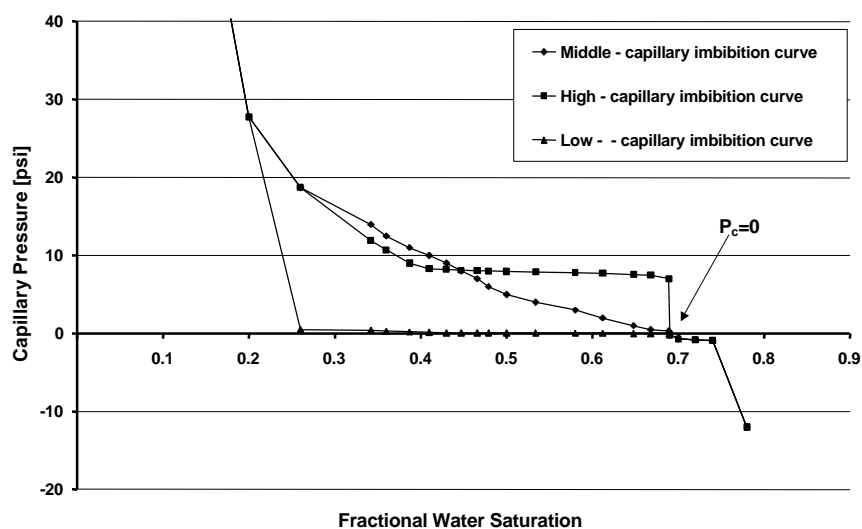


Figure 10. Three alternative representations of the positive capillary pressure imbibition curve for $I_w = 0.8$.

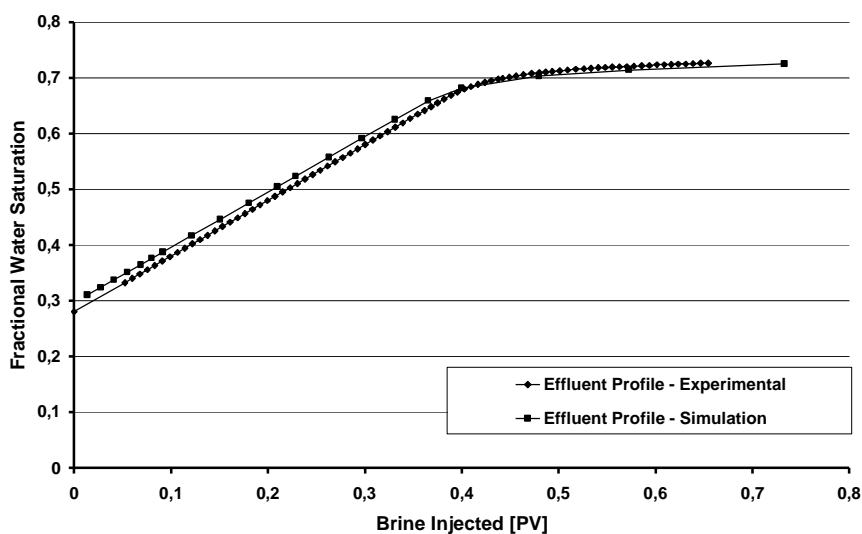


Figure 11. Experimental and simulated average water saturations when waterflooding the whole block CHP8. The medium capillary pressure curve is used.

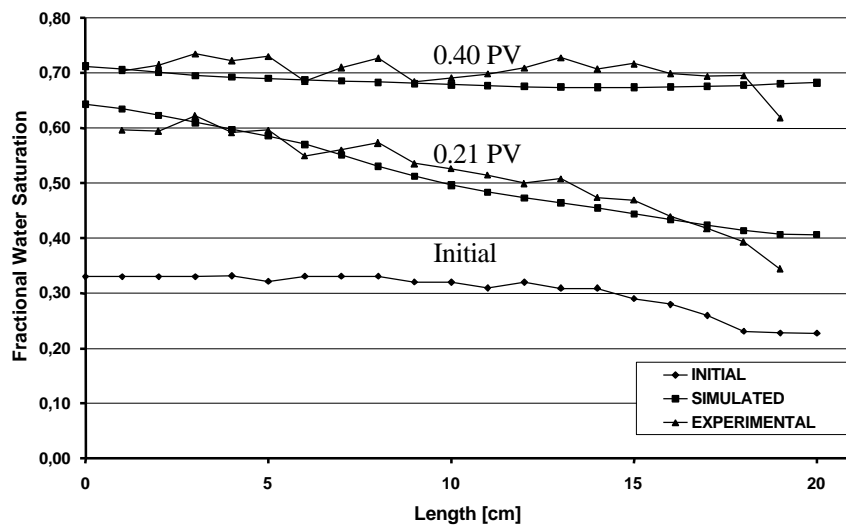


Figure 12. Experimental and simulated water saturation profiles, averaged over the cross section of the block, when waterflooding the whole block CHP8. The medium capillary pressure curve is used.